

# Enhanced coupling of electronic and photonic states in a microcavity-quantum dot system

M. Gerlach<sup>\*,a</sup>, Y. P. Rakovich<sup>a</sup>, J. F. Donegan<sup>a</sup>, N. Gaponik<sup>b</sup>, A. L. Rogach<sup>c</sup>

<sup>a</sup>Semiconductor Photonics Group, Department of Physics, Trinity College Dublin, Dublin 2, Ireland

<sup>b</sup>Institute of Physical Chemistry, University of Hamburg, 20146 Hamburg, Germany

<sup>c</sup>Department of Physics and CeNS, Ludwig-Maximilians-Universitaet Muenchen, 80799 Munich, Germany

## 1. ABSTRACT

Spherical microcavities consisting of a dielectric material show unique optical characteristics as resonators in combination with semiconductor nanoparticles. A high quality factor results in a very narrow bandwidth of the resonant modes (whispering-gallery modes) inside the microcavity. The polystyrene microspheres are coated with one monolayer of CdTe nanocrystals which offer a high photostability and a high quantum yield at room temperature. Due to strong confinement of the electrons in all three dimensions, excitation from the quantum dots is highly size-dependent and tuneable over almost the whole visible spectrum. The deposition of the nanocrystals on the sphere surface allows efficient coupling of the light of the CdTe quantum dots into the microcavity. Photoluminescence and Raman spectra were taken with a Renishaw Raman system. The setup is equipped with an Ar<sup>+</sup>-laser and a HeNe-laser to excite the nanocrystals. Raman measurements show a series of very sharp resonant peaks instead of a continuous spectrum. Strong interaction between the electronic states of the nanocrystals and the resonant modes in the microsphere causes a considerable enhancement of the Raman scattering and luminescence from the CdTe quantum dots in Stokes and anti-Stokes region. Furthermore, a linear blue shift of the resonances in the photoluminescence spectrum was observed during continuous excitation for 18 minutes with a HeNe laser.

Keywords: Raman scattering, photoluminescence, spherical microcavity, microsphere, nanocrystals, quantum dots

## 2. INTRODUCTION

Spherical microcavities in the micrometer regime show unique properties as three-dimensional optical resonators. Strong feedback inside the cavity offers ideal conditions for linear and nonlinear processes [1]. Polymer latex microspheres coated or doped with semiconductor nanocrystals are studied in recent years to develop microlaser [2] based on Raman scattering or photoluminescence (PL) of the quantum dots (QDs). A very high quality factor (Q) and small mode volume of the spherical microcavity result in a very narrow bandwidth. The emission spectrum of the QDs is tuneable over a large spectral range by using nanocrystals with different diameter. Our samples consist of CdTe QDs deposited on the microsphere surface. The narrow peaks of the whispering-gallery modes (WGM) in the Raman or PL spectrum can be measured and detailed studies such as decay lifetime of the electronic states [3] or lasing [3,4] can be carried out. Other potential applications for microsphere resonators are microsphere sensors for probing the sphere environment due to the high sensitivity of the frequency of the resonant modes to changes in temperature, pressure and chemical composition at the sphere surface. Microspheres can also be used for narrowing the linewidth of diode laser as well as frequency locking and stabilization without explicitly increasing the dimensions of the laser. Further potential applications could be in the area of optical filters, e.g. add/drop-filters or in the non-linear optics domain such as two photon absorption.

## 3. BASIC PRINCIPLES

The so called whispering-gallery modes are electromagnetic resonances inside of the microsphere which occur only at discrete wavelengths. These resonant modes depend on the refractive index and the radius of the sphere. The light which is coupled into the sphere travels around the equator close to the surface caused by total internal reflection inside the sphere. Apart from the circular trajectory the light also travels on a zig-zag path. To distinguish between the modes they

are characterised by three mode numbers, the radial mode number  $n$ , the angular mode number  $l$  and the azimuthal mode number  $m$ . The angular mode number  $l$  is close to the number of wavelengths which fit into the circumference of the equator. The value of  $l-|m|+1$  is equal to the number of field maxima in polar direction, perpendicular to the equatorial plane. The radial mode number  $n$  specifies the number of field maxima in the radial direction. The negative or positive value of  $m$  describes the opposite directions of travel of the light inside the sphere. The different values of  $m$  characterise the inclination angles of the zig-zag path with respect to the equatorial plane. All modes with the same  $l$  and  $n$  have the same resonant wavelength while the value for  $m$  can vary from 0 up to  $l$ .  $m = l$  defines the fundamental mode in the sphere with the smallest amplitude of the zig-zag path. The other factor which defines the characteristics of WGMs is the polarisation. There are two possible polarisation states, the transverse-electric (TE) and the transverse-magnetic (TM) mode. These modes have an electric and a magnetic field vector which is normal to the direction of propagation. In the case of TE-modes the electric field vector is perpendicular to the equatorial plane of the sphere and in the case of TM-modes the magnetic field vector is perpendicular to the equatorial plane. The reason for the fact that only TE and TM modes exist in microspheres lies in the behaviour of the light at the boundary between the medium of the sphere and the outer medium. It also results in a phase shift between TE and TM modes and therefore in a separation in the spectrum of the modes with the same mode numbers. The calculation of the whispering-gallery modes was discussed in detail by G. Mie in 1908 for the first time [5]. The WGM-spectrum of a microsphere can be computed either from the Maxwell equations with appropriate boundary conditions or from quasi-bound states of a Schrödinger-like equation. The active material in the microcavity-quantum dot system is CdTe. With a diameter of only a few nanometer, the quantum dots strongly confine the electronic states in the semiconductor in all three dimensions. As a result, the bandgap energy is a function of the size of the QDs. Thus, the emission from the QDs is also tuneable over a broad spectral range due to recombination of the excited electrons in the nanocrystals. The CdTe nanocrystals in our samples are tuneable from approximately 510 nm for QDs with 2nm diameter up to 730 nm for QDs with a diameter of 6 nm, respectively. The PL spectrum shows inhomogeneous broadening due to size distribution of the QDs on the microsphere surface.

#### 4. EXPERIMENTAL METHOD

Our samples consist of polystyrene microspheres with a diameter of 70  $\mu\text{m}$  commercially available at Micro Particles GmbH (Berlin, Germany). The semiconductor colloidal CdTe nanocrystals with a diameter of 4.8 nm have a PL maximum at 620 nm wavelength. The QDs feature a high photostability due to a capping layer of thioglycolic acid and a PL quantum efficiency of about 25% at roomtemperature. The microsphere surface is coated with the CdTe QDs using a layer-by-layer technique as described in [6]. As the CdTe nanocrystals are negatively charged, a polyelectrolyte layer is first applied on the sphere surface to increase the electrostatic force which attracts the nanocrystals on the surface. One monolayer of CdTe QDs is deposited on the microsphere which is similar to a close-packed thin-film layer of CdTe QDs. A Si wafer is used as a substrate for the samples. The silicon LO phonon mode at  $520\text{ cm}^{-1}$  also works as a built-in reference for all measurements. At first, the absorption and PL spectra of the colloidal QDs in water were measured with a Shimadzu-3101 and Spex Fluorolog spectrometer, respectively. The Raman and PL measurements were carried out with a computer controlled Renishaw micro-Raman setup ( $\sim 1800\text{ mm}^{-1}$  grating,  $1\text{ cm}^{-1}$  resolution) equipped with a  $\text{Ar}^+$ - and HeNe-laser as excitation sources. In this setup the laser light is focused through a microscopic lens on the sample and the scattered light is collected through the lens and guided to a spectrometer. The samples are placed on a piezo-stage for accurate movement in all three directions. The Raman and PL spectrum of the sample can be measured with a spatial resolution of around 0.5  $\mu\text{m}$  depending on the spot-size of the focused excitation laser beam. The microsphere samples are kept in an alcoholic solution. To lower the concentration of the microspheres, the solution is diluted in a separate beaker first. For preparing the measurements, some microliters of the solution containing the microspheres is dropped on the si-substrate with a pipette. After the alcohol evaporated the substrate is placed on piezo stage in the Raman setup. Using the microscope equipped with a CCD camera, the laser is focused accurately at the required position on the sphere. The light coupled into the sphere with a Gaussian shaped focused laser beam is less efficient than coupling via evanescent field but it is a rather convenient coupling method because no complicated preparation and adjustment of the system is required as it is for the prism [7] or tapered fibre coupler [8]. Prior to the measurement, the excitation source is chosen. The HeNe laser is working at 632.8 nm, the  $\text{Ar}^+$  laser at 488 nm or 514 nm. After setting up the laser, the proper notch plasma filter which filters out the laser line from the spectrum is placed into the system. In the next step, the system is aligned to optimize the spot size of the focused laser beam. The main parameters to choose from are the spectral range to measure, the integration time to reduce noise and the type of measurement which is either

Raman scattering or photoluminescence. After this, the laser is focused on the sample. It is possible to choose between several microscope lenses in the range of 5X up to 100X magnification. The recorded spectrum is converted into an ascii file for further processing of the data. For taking the spectrum during continuous excitation, the shutter for the laser beam was left open and the scan was started approximately every 30 seconds.

## 5. RESULTS

At first, the absorption and PL spectra of colloidal CdTe quantum dots in water were measured. The pump source was the  $\text{Ar}^+$  laser exciting at 488 nm and 2 mW output power. The absorption and PL graph is shown in Fig. 1. As expected, strong confinement of the electronic states in all three dimensions results in a blue shift of the absorption maximum by nearly 610 meV in relation to the bulk CdTe semiconductor material. The pronounced maximum in the absorption graph corresponds to the first excited state in the nanocrystal. The PL maximum is situated at around 622 nm showing a redshift in respect to the absorption peak at around 592 nm. In the following measurement, the Raman spectrum of bulk polystyrene material and a single PS microsphere coated with one monolayer of QDs was taken. A  $\text{Ar}^+$  laser at 488 nm wavelength and 2 mW output power was used to excite the nanocrystals on the sphere surface. We have chosen two different focus positions on the microsphere. In the first measurement, we focused the beam in the center of the sphere and in the second measurement at the rim of the sphere. One spectrum was taken from a bulk polystyrene film on a plane substrate as a reference. The graphs are shown in Fig. 2 a). In agreement with the theory [9], the overall intensity of the spectrum when excited at the rim of the sphere is higher compared to the intensity when excited in the sphere center.

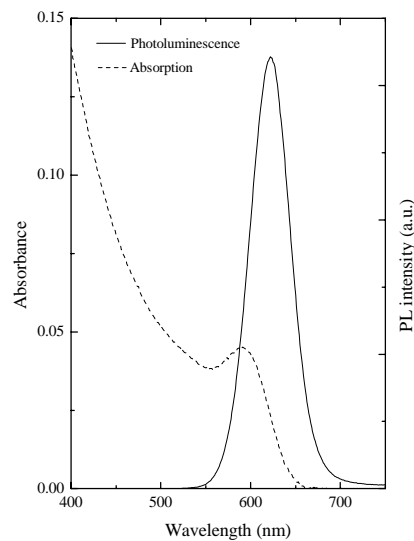


Fig. 1. Absorption and photoluminescence spectrum of colloidal CdTe quantum dots in water.

The reason for that is the higher efficiency of coupling light into the resonant modes of the microcavity close to the surface when the laser beam hits the sphere almost tangential to the surface. The spectrum of the polystyrene film on a glass substrate shows several Raman modes intrinsic to polystyrene. All three measurements show the LO phonon mode of silicon at  $520 \text{ cm}^{-1}$ . The highest intensity of this peak is in the third measurement where the beam passes the sphere at

the rim and reflected back directly from the substrate. Apart from the Raman peaks, the high intensity of the background is due to the photoluminescence of the quantum dots which emit a photon caused by recombination of the confined electrons in the nanocrystals. Taking a closer look at the broad peak at around 493 nm reveals a remarkable observation. The peak is composed of a LO phonon mode (492 nm) of CdTe and a Raman mode (493.3 nm) of polystyrene. The Lorentzian fit of both single peaks is shown in Fig. 2 b) (dashed lines).

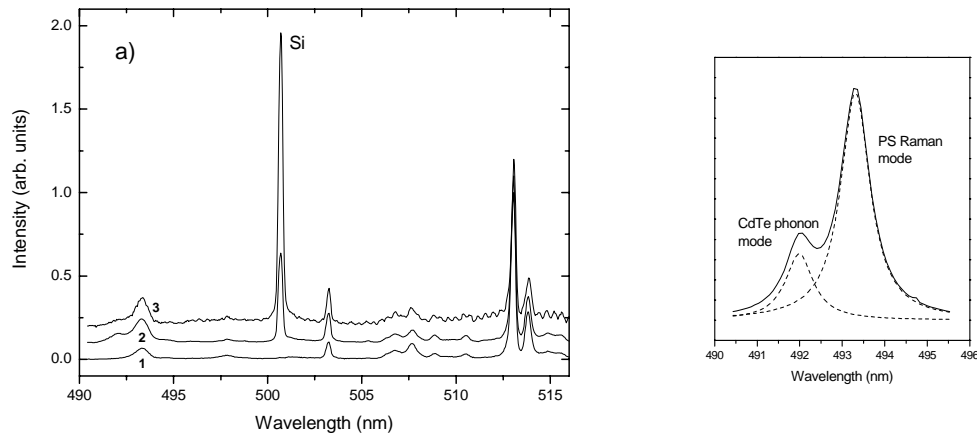


Fig. 2. a) Raman spectrum of: (1) bulk polystyrene film on glass substrate.  
 (2) PS microsphere/CdTe quantum dots excited in the sphere center.  
 (3) PS microsphere/CdTe quantum dots excited at rim of sphere.  
 b) Lorentzian fit of CdTe LO phonon (492 nm) mode and PS Raman mode (493.3 nm).

As a result of the strong interaction between the confined electronic states of the nanocrystals and the optical resonant modes of the microcavity, it was possible to observe Raman scattering from a CdTe QD layer of less than 5 nm. The optical feedback inside the microsphere strongly increases the intensity of a Raman signal and thus considerably increasing the sensitivity of the detection system indirectly. The other remarkable fact in the Raman spectrum is the ripple structure appearing when excitation is at the rim of the microsphere.

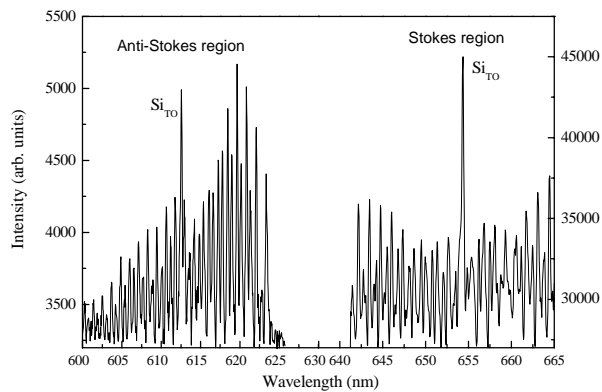


Fig. 3. Raman spectrum showing the whispering-gallery mode structure of the 70  $\mu\text{m}$  polystyrene microsphere coated with CdTe quantum dots.

This ripples are the resonant modes of the microcavity. The optical confinement inside the microsphere results in a whispering-gallery mode peak structure. The background intensity is caused by reflected light which is not coupled into the sphere. The intensity of the WGMs decreases towards the excitation wavelength probably due to stronger absorption of the CdTe nanocrystals [10] (Fig. 1). In the following measurement, the samples were excited with the HeNe laser at 632.8 nm. Now, the excitation energy is below the first absorption band of CdTe. The spectrum is shown in Fig. 3. It reveals the sharp peaks of the WGMs instead of a continuous intensity distribution over the whole spectral region. The high Q-factor of a spherical microcavity results in very narrow resonance peaks. The intensity below the excitation energy of the HeNe laser (anti-Stokes region) is exceptionally high in this measurement. It is only one order of magnitude below the intensity of the signal in Stokes region. Such strong anti-Stokes excitation requires high quantum efficiency of the semiconductor QDs [11,12]. It is important to notice that the signal is photoluminescence from the CdTe QDs although it is a Raman-type measurement. Again, the feedback of the optical signal inside the microcavity strongly increases the intensity of the light emitted from the nanocrystals and coupled into the microsphere. The measured spectrum also shows a sinusoidal-shaped intensity fluctuation of the resonant modes. This effect is caused by interference of the light between the bottom and the top of the microsphere [13]. The spacing between the resonant modes mainly depends on the refractive index of the sphere and the surrounding medium as well as the radius of the microsphere. Changes of the WGM mode structure can be induced by a change of these parameters. The free spectral range between the WGMs depends mainly on the size of the microsphere. The mode spacing  $\Delta\lambda$  of two adjacent modes with the same polarisation can be approximated by the equation

$$\Delta\lambda = \frac{\lambda^2 \tan^{-1} \{n^2 - 1\}^{\frac{1}{2}}}{\pi d \{n^2 - 1\}^{\frac{1}{2}}},$$

where  $n$  is the refractive index and  $d$  the diameter of the microsphere. A Fourier transformation was used to analyse the spacing in the measured photoluminescence spectrum. The PL spectrum was divided into two parts in case that there is a strong wavelength dependency of the spacing. The first Fourier transformation was carried out within the spectral region between 640 nm and 655 nm, the second one between 655 nm and 670 nm. The Fourier spectrum is directly related to the spacing of the resonant modes, in fact it shows the inverse spacing of the WGMs averaged over the spectral range. Four spectra are evenly picked out of the timeframe of excitation and the Fourier transformation is determined (Fig. 4). The peak positions in the Fourier spectrum give the inverse value of regular spacing in the WGM spectrum. The first peak in the Fourier graph belongs to the spacing between two modes, either TE or TM, of the same polarisation. As the spacing between two TE modes is almost the same as between two TM modes, you can only see one peak in the Fourier spectrum. The double peak at around  $1.5 \text{ nm}^{-1}$  belongs to the spacing between a TE and TM mode with the same mode order  $l$  and the spacing between a TE and TM with a mode order  $l$  and  $l+1$  respectively. The first peak of the 10% intensity measurement for the first part of the PL spectrum is at  $0.794 \text{ nm}^{-1}$  which corresponds to a mode spacing of  $\Delta\lambda=1.260 \text{ nm}$ . Calculations based on the equation above give a theoretical value of  $\Delta\lambda=1.305 \text{ nm}$  for  $\lambda=644.5 \text{ nm}$  which is in between the range of the Fourier transformation. For the second part of the PL spectrum, the spacing is  $\Delta\lambda=1.389 \text{ nm}$  and the calculated value is  $\Delta\lambda=1.380 \text{ nm}$  for  $\lambda=662.5 \text{ nm}$ . Both values are in good agreement with the measurements. The result shows a strong wavelength dependency of the spacing of the WGMs. In each graph, the peak position doesn't change in the four spectra taken at different times during excitation with the pump HeNe laser. That means that the spacing is constant over time within the accuracy given by the analysis of the spacing with the Fourier transformation. However, the accuracy is limited because the spacing is only an average of all the modes within the range of the PL spectrum of the transformation. For a more accurate analysis, seven random resonant modes from the measured spectrum were taken and the distance to the adjacent mode was determined as a function of excitation time. The analysis shows a very small decrease of the spacing within the excitation time of  $T=1060$  seconds of  $\Delta\lambda=0.003 \text{ nm}$  for all seven resonant mode pairs. To investigate the influence of long-time exposure of the microspheres/QDs to the laser light, we excited the sphere for a time period of 18 minutes in the Raman setup. The PL spectrum was taken approximately every 30 seconds during continuous excitation. The HeNe laser with reduced output power of 3 mW was used as the pump source. Two data series were taken in this measurement. One with full laser output power and one with 10% output power lowered with neutral density filter. The samples are the same  $70 \mu\text{m}$  polystyrene microspheres on a silicon substrate as in the previous measurements. The intensity was integrated over the whole spectral range for each PL spectrum. Plotting the integrated

PL intensity versus the exposure time shows an exponential decay of the PL intensity. The reason for this is the photodegradation mechanism which reduces the emission of light from the QDs significantly. There is no full understanding of the photodegradation process yet. Recent studies on this subject assume two processes occurring in nanocrystal semiconductor material. One process is a chemical modification of the QD surface or of the polyelectrolyte layer. Defect states on the surface can quench the photoluminescence intensity due to non-radiative recombination of the charge carriers. Another explanation could be the reversible process of Auger autoionisation

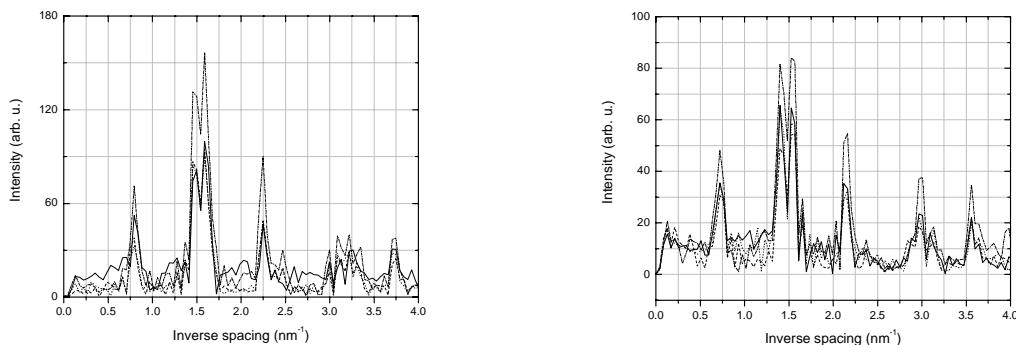


Fig. 4. Fourier spectrum of the first and the second half of the photoluminescence spectrum at 10% laser intensity for four measurements taken during excitation.

in which charged exciton states quench the photoluminescence of the nanocrystals [14]. The free charge carrier in the quench the excitation by non-radiative energy transfer. Due to a limited lifetime of the charged electronic states, the luminescence intensity can recover over time. To study the effect of continuous excitation on the resonant modes, the position of two particular WGMs was plotted versus the excitation time. The resonant modes were chosen from the lower and the higher end within the range of the measured PL spectrum. The two graphs in Fig. 5 show the shift of the two actual resonant modes over the excited time period for the measurement at the reduced 10% power setting and Fig. 6 at 100% laser output power. The step-like gradient of the graphs originates from the limited resolution of the spectrometer. All graphs show a linear blue shift of the particular mode during excitation with the HeNe laser. The slope of the graph determined by a linear fit is the shifting speed of the mode. For the 10% output power measurements the shifting speed  $v_{10,1} = -7.496 \cdot 10^{-4}$  nm/sec and  $v_{10,2} = -7.572 \cdot 10^{-4}$  nm/sec, respectively. The shifting speed for the 100% power measurement is  $v_{100,1} = -4.376 \cdot 10^{-4}$  nm/sec and  $v_{10,2} = -4.615 \cdot 10^{-4}$  nm/sec, respectively. The resonant modes in the 10% measurement shift almost twice as fast as in the 100% measurement. It is also slightly slower at shorter wavelengths at the same excitation power which might be caused by the refractive index dispersion of the microsphere medium. The constant shift of the WGMs could be explained by a change of the nanocrystal properties on the sphere surface as well as a thermal process due to heating of the polystyrene microsphere. Expansion of the microsphere produces a redshift of the modes while contraction causes a blueshift in the resonance mode spectrum. Due to the fact that the polystyrene microsphere expands with increasing temperature, the blue shift could not be explained by the thermal effect. The blue shift is probably induced by the nanocrystal layer on the surface. It is well known that the resonances are very sensitive to changes on the microsphere surface. In recent years, research was concentrated on protein detection with microsphere sensors due to the shift of the WGMs [15, 16]. Very small amounts of material on the sphere surface can result in a shift of the resonances. Furthermore, a change of the refractive index of the coated material as well as the surrounding medium causes a resonant shift. In our samples, the CdTe nanocrystals presumably have their properties such as the refractive index changed during continuous excitation with the HeNe laser, causing the linear shift of the WGMs. Further measurement should clarify if the nanocrystals are permanently damaged or if there is a recovery when the samples are no longer excited over a longer time period. Further experiments are planned to investigate if the CdTe coated microspheres can be used for protein or gas detection. The slope of the graph which corresponds to the shifting speed could be a new variable to sense the sphere environment with high sensitivity. CdTe nanocrystals coated on a spherical microcavity lead to a strong enhancement of interaction between resonances (WGMs) in the microsphere and the CdTe nanocrystals on the sphere surface. The observation of a LO phonon mode in one

monolayer of CdTe was possible as well as a strongly enhanced contribution of photoluminescence in the Stokes- and anti-Stokes region of the Raman spectrum measurements. Microspheres significantly increase the sensitivity for detecting weak Raman scattering and photoluminescence emitted by the nanocrystals. The broad PL spectrum indicate great potential for widely tuneable microsphere laser with a particularly narrow bandwidth due to the high Q factor of the spherical microcavity. Applying different nanocrystal sizes allows us to cover almost the whole visible range and the near infrared region with CdTe quantum dots.

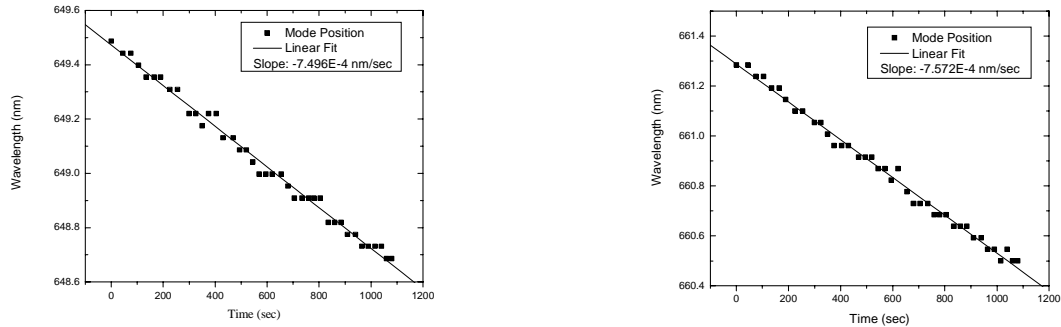


Fig. 5. Blue shift of resonant modes versus excitation time during continuous excitation with the HeNe laser at 10% output power.

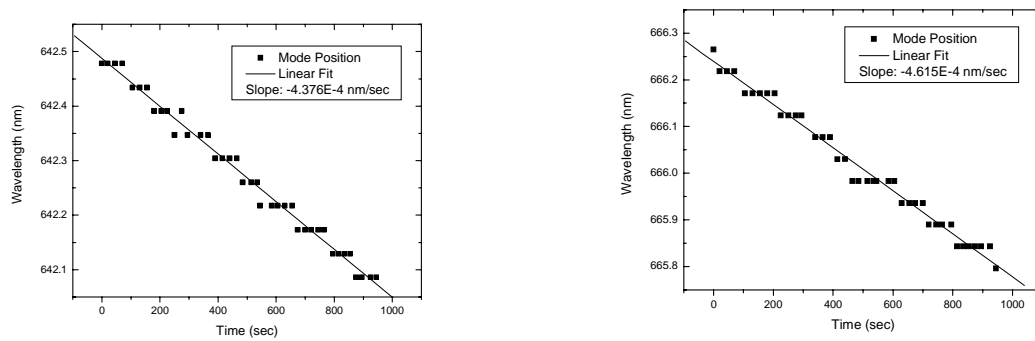


Fig. 6. Blue shift of resonant modes versus excitation time during continuous excitation with the HeNe laser at 100% output power.

## 6. CONCLUSIONS

In conclusion, we observed a strong interaction between the confined electronic states of the nanocrystals and the resonances of the spherical microcavity due to the feedback of the light trapped inside the sphere. As a result, a LO phonon mode of one monolayer of 4.8 nm QDs was clearly detected with the Raman setup. Strong PL emission in Stokes and anti-Stokes region was measured simultaneously by low excitation with a HeNe laser below the bandgap of CdTe. Resonance peaks with a narrow bandwidth were measured over a broad spectral range offering potential for widely

tuneable microsphere laser in almost the whole visible electromagnetic spectrum. By changing the size of the microcavity, the spacing between the resonant modes is also tuneable for adaptation to various requirements, for example in the telecommunication sector for high optical data transfer in dense wavelength multiplexing. The photodegradation effect revealed a strong exponential decrease of intensity over time. A linear shift of the WGMs during continuous excitation with the HeNe laser was observed. The shifting speed of the resonances depended on the excitation power and the spectral position of the WGM. Although further theoretical investigations are required in terms of the correlation between the mode shifting and the photobleaching of the CdTe nanocrystals, the observed effect enables potential fine tuning of WGMs depending on the irradiation time. The advantage of this approach can be applied in microsphere-sensor bioapplications to monitor the presence of extremely small quantities of proteins and oligonucleotides on the surface of the microsphere.

## ACKNOWLEDGEMENTS

This work was supported by Science Foundation Ireland under grant number 02/IN.1/I47 and by the Deutsche Forschungsgemeinschaft through the SPP 'Photonic Crystals'.

## REFERENCES

1. K.J. Vahala, *Nature* 424 (2003) 839–846.
2. S.M. Spillane, T.J. Kippenberg, K.J. Vahala, *Nature* 415 (2002) 621–623.
3. M.V. Artemyev, U. Woggon, R. Wannemacher, H. Jaschinski, W. Langbein, *Nano Lett.* 1 (6) (2001) 309–314.
4. V.I. Klimov, M.G. Bawendi, *MRS Bull.* 26 (12) (2001) 998–1004.
5. G. Mie, *Ann. Phys.* 25, 377 (1908).
6. A.S. Susha, F. Caruso, A.L. Rogach, G.B. Sukhorukov, A. Kornowski, H. Moehwald, M. Giersig, A. Eychmueller, H. Weller, *Col. Surf. A* 163 (2000) 39–44.
7. M. L. Gorodetsky, V. S. Ilchenko, *J. Opt. Soc. Am. B.* 16, 147 (1999).
8. S. M. Spillane, T. J. Kippenberg, O.J. Painter, K. J. Vahala, *Phys. Rev. Lett.* 91, 043902/1 (2003).
9. A. Serpenguzel, S. Arnold, G. Griffel, J.A. Lock, *J. Opt. Soc. Am. B* 14 (4) (1997) 790–795.
10. Yu. P. Rakovich, L. Yang, E. M. McCabe, J. F. Donegan, T. Perova, A. Moore, N. Gaponik, A. Rogach, *Semicond. Sci. Technol.* 18, 914 (2003).
11. K.I. Rusakov, A.A. Gladyschuk, Yu.P. Rakovich, J.F. Donegan, S.A. Filonovich, M.J.M. Gomes, D.V. Talapin, A.L. Rogach, A. Eychmueller, *Opt. Spectros.* 94 (6) (2003) 921–925.
12. X. Wang, W.W. Yu, J. Zhang, J. Aldana, X. Peng, M. Xiao, *Phys. Rev. B* 68 (2003) 125318.
13. Petr. Chylek, Jiyu Zhan, *J. Opt. Soc. Am. A* 6, 1846 (1989).
14. F. Huisken, D. Amans, G. Ledoux, H. Hofmeister, F. Cichos, J. Martin, *New J. of Physics* 5, 10.1–10.10 (2003).
15. S. Arnold, M. Khoshima, I. Teraoka, S. Holler, F. Vollmer, *Optics Lett.* 28, 272 (2003).
16. F. Vollmer, S. Arnold, D. Braun, I. Teraoka, A. Libchaber, *Biophysical Journal* 85, 1974 (2003).

\* [gerlachm@tcd.ie](mailto:gerlachm@tcd.ie); phone: +353 (0)1 608 2167; fax: +353 (0)1 671 1759; [www.tcd.ie](http://www.tcd.ie)